

DETERMINATION OF INPUT/OUTPUT CHARACTERISTICS OF FULL-BRIDGE AC/DC/DC CONVERTER FOR ARC WELDING

Assist. prof. Dr. Eng. Stefanov G.¹, Prof. Dr. Eng. Karadzinov Lj.², Assos. prof. Dr. Eng. Sarac V.³, Prof. Dr. Eng. Cingoski V.⁴,
Assos. prof. Dr. Eng. Gelev S.⁵

Faculty of Electrical Engineering-Radovis, University 'Goce Delcev'-Stip, Macedonia^{1,3,4,5}
FEIT, University Sv. Kiril and Methodius -Skopje, Macedonia²

goce.stefanov@ugd.edu.mk, L.Karadzinov@feit.ukim.edu.mk, vasilija.sarac@ugd.edu.mk, vlatko.cingoski@ugd.edu.mk,
saso.gelev@ugd.edu.mk

Abstract: This paper describes the design and practical implementation of AC/DC/DC converter in mode of arc welding. An analysis of the operation of AC/DC/DC converter and its input/output characteristics are determined with computer simulations. The practical part is consisted of AC/DC/DC converter prototype for arc welding with output power of 3 kW and switching frequency of 64 kHz. The operation of AC/DC/DC converter is validated with experimental measurements.

Keywords: DC/DC CONVERTER, COMPUTER SIMULATIONS, EXPERIMENTAL MEASUREMENTS, WELDING, EFFICIENCY

1. Introduction

In power converters such as switches generally are used IGBT and MOSFET transistors. The decision which of them will be chosen depends on the specific application.

The IGBT transistors are preferred to MOSFETs in high power range applications due to its ability to higher power density conversion. IGBT transistors are designed for higher rated voltages and currents and have lower conduction losses compared to MOSFETs. However, the IGBTs are slower than MOSFETs because of higher switching losses which come from the tail current at turn-off. Hence, if the IGBT transistor is used for higher switching frequencies the turn-off losses should be minimized. A solution may be either zero voltage switching (ZVS), which is effected by adding an external snubber capacitor or zero current switching (ZCS). Zero current switching seems to be more efficient than zero voltage switching since the tail current problem can be minimized by removing the minority carriers before turning off [1], [2], [3], [4]. Most of full-bridge AC/DC/DC converters are controlled by Phase-Shifted PWM scheme [5], [6], [7], [8]. In this paper, for full-bridge DC/DC converter with defined output load, are made computer simulations for estimation of switching losses of IGBT transistors. Practically AC/DC/DC converter is designed and implemented for arc welding and input/output characteristics are obtained.

In this paper in Section II an overview of operating principle of full-bridge DC/AC converter will be represented. Section III is given design of AC/DC/DC convertor with computer simulations. Input/Output characteristics of the convertor are obtained experimentally and are represented in Section IV. Section V concludes this paper.

2. Operating Principle on Full-Bridge DC/AC Power Converter

The conventional DC/DC converter operates with PS-PWM control at constant switching frequency. The output current is controlled by change of the phase shift between (transistors T1, T4) and lagging leg (transistors T2, T3), as given in the Fig. 1. Basically, the full-bridge DC/DC converter is based on the operation of the DC/AC converter.

In this part it is analyzed state when the DC/AC converter operates in conditions of inclusion of switches with ZVS [8]. In Fig. 1 is shown the electrical scheme of this full-bridge DC/AC converter. The converter DLink voltage is $V_{dc} = 300$ V DC and the switching frequency is $f_s = 64$ kHz. The used switches are insulated gate bipolar transistor module (IGBT) type IRGP50B60PD1-E with anti-parallel ultrafast recovery diode. Their on-state voltages are $V_{cesat} = 2$ V and $V_D = 1.3$ V for the IGBT and anti-parallel diode.

The output current is lagging in respect with the output voltage. This analyze presents converter operation only in the steady-state,

that is, all converter currents and voltages have the same values at the end of each period as at its beginning.

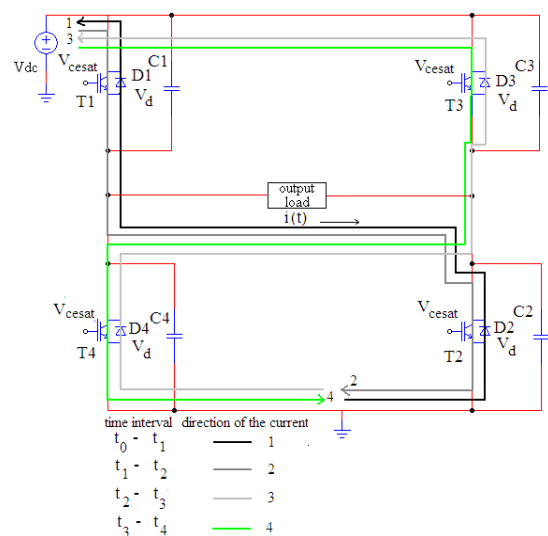


Fig. 1. Full-bridge DC/AC converter topology and the steady-state current paths in all four time intervals during one period.

During one switching period $T = 1/f_{sw}$ there are four time intervals determined with the switching on and off of the IGBTs and anti-parallel diodes. So, output converter voltage changes during operation in the four time intervals: $t_0 - t_1$, $t_1 - t_2$, $t_2 - t_3$, $t_3 - t_4$.

Analysis of the Converter Operation

Depending on switches on/off-state, output converter current has different paths for each of the four intervals shown in the Fig. 1.

1. Time interval $t_0 - t_1$. In this interval the diodes D1, D2 are turned-on. The output current direction is shown with the line 1 in the Fig. 1. The output converter current is returning power to the DC link voltage source. The transistors T1, T2, T3, T4 are turned off.

2. Time interval $t_1 - t_2$. Now the transistors T1 and T2 are turned on. The output current direction is now shown with line 2. The current is supplied from the DC link voltage, through the output load to ground. The transistors T1 and T2 turn-on at zero-voltage (ZVS), since until the moment t_1 the diodes D1 and D2 are turned-off.

3. Time interval $t_2 - t_3$. At the moment t_2 the transistors T1 and T2 turn-off, and the transistors T3 and T4 are not yet turned-on. Now, the output converter current is flowing through the diodes D3 and D4 returning power to the DC link voltage. The output current direction is shown with the line 3 in the Fig. 1.

4. Time interval $t_3 - t_4$. In this time interval the transistors T3 and T4 are turned-on. The converter output current is supplied from the DC link voltage through the output load to the ground. The output current direction is shown with line 4 in Fig. 1.

3. Design of Full-Bridge AC/DC/AC Power Converter with Computer Simulations

In this section, computer simulations in PowerSim [9] program are performed in order to estimate the switching losses of IGBT transistors in full-Bridge DC/AC converter. With the simulations the input power, harmonic distortion of voltage and current, input effective current and converter output power are determined. Also, calculation are made for efficiency of the converter for different widths on the pulse at the gates of the IGBT transistors in the bridge.

Estimate the Switching Losses of IGBT Transistors in Full-Bridge AC/DC/DC Power Converter

In the Fig. 2 is shown circuit of a full-bridge DC/DC converter used for computer simulations in PowerSim program. The parameters of the elements are shown in the Fig. 2. With this parameters and switching frequency $f = 64 \text{ kHz}$ the converter output power is $P_o = 3.091 \text{ kW}$.

In the Fig. 3 are shown waveforms of the current $i_c(t)$, voltage collector-emitter $u_{CE}(t)$ and power losses $p_{Tz}(t)$ of one IGBT transistors module (transistor with anti-parallel diode) in bridge.

In the Fig. 3 also is shown the size of switching losses. The switching losses during turn-on period are less than switching losses during turn-off period. Turn-on of transistor is soft, i.e. the transistor is switched by ZVS, and turn-off transistors is hard, i.e. current flows through it at the moment of this switching period.

In the Table I are given maximum and average value of the collector-emitter voltage when the IGBT transistor is turn-off, maximum and average value of its collector current and power losses of one IGBT module.

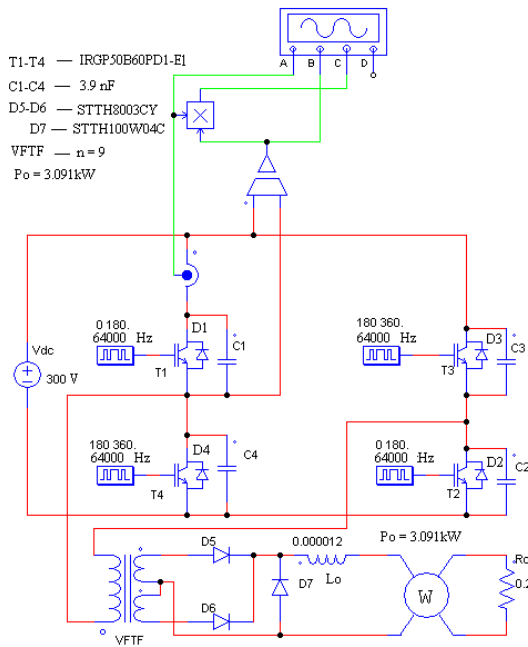


Fig. 2. Circuit of full-bridge DC/DC power converter used for computer simulations in the PowerSim program.

From Fig. 2 and Table I can be concluded that maximum collector-emitter voltage $v_{CE}(t)$ of IGBT transistors is 297.7 V. Maximum collector current $i_c(t)$ is 15.6 A while maximum power losses of the IGBT transistors module is 14.65 W.

The main conclusion from this simulations is that in application of DC/DC converter with output power $P_o = 3.091 \text{ kW}$, current-

voltage load and power losses of IGBT modules in the bridge are smaller and the proposed IGBT (IRGP50B60PD1-E) transistors operates satisfactory.

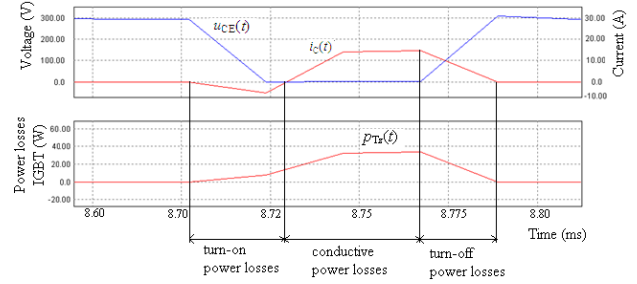


Fig. 3. Waveforms of $i_c(t)$, $v_{CE}(t)$ and $p_{Tz}(t)$ of one IGBT transistors module in bridge.

TABLE I: $V_{CE}(T)$, $I_C(T)$ AND $P_{Tz}(T)$ OF IGBT MODULE

v_{CE} [V]	i_C [A]	P_{Tz} [W]
max	max	average value
297.7	15.6	14.65

Determination of Input/ Output Characteristic on Full-Bridge AC/DC/DC Power Converter

Simulations circuit is the same as in Fig. 2, with that the source of DC power supply is replaced with the mains voltage with an effective value 220 V and frequency 50Hz and 30A single phase bridge rectifier module (MDQ 30A). The power transformer VFTF is with parameters: magnetizing inductance $L_m = 2.85 \text{ mH}$, primary leakage inductance $L_L = 3.4 \text{ μH}$, transformer turns ratio $n = 9$, smoothing inductance: $L_0 = 12 \text{ μH}$. In the simulations is used resistor with value $R_0 = 0.2 \text{ Ω}$ [10], [11], [12]. The output voltage of the unloaded converter is 60 VDC.

In the Fig. 4 are shown waveforms of the input current $i_{in}(t)$, input voltage $V_{in}(t)$ and input power $P_{in}(t)$, and in Fig. 5 are shown harmonic amplitude specter of the input current and input voltage. This waveforms are obtained for maximal output power 3.091 kW.

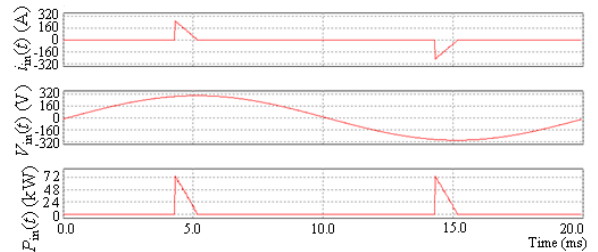


Fig. 4. Waveforms of $i_{in}(t)$, $V_{in}(t)$ and $P_{in}(t)$ when output power is maximal 3.091 kW obtained by simulations in PowerSim program.

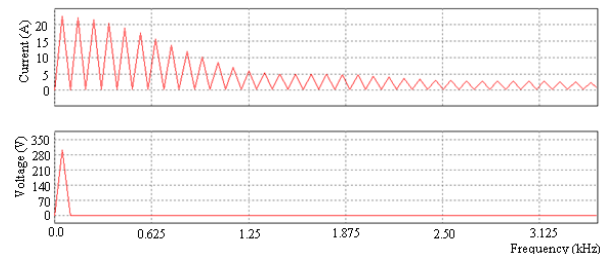


Fig. 5. Harmonic amplitude specter of the input current and input voltage when output power is maximal 3.091 kW.

From Fig. 4 and Fig. 5 can be seen that input voltage has sine form without harmonic in the specter, as and that input current is distortion with high order harmonics in the specter. In Table II are given the values for the effective input current I_{in} , effective input voltage V_{in} , total harmonics distortion of the input current THDC and power factor PF obtained with simulations for maximal output power 3.091 kW.

TABLE II: VALUES FOR I_{IN} , V_{IN} , $THDC$ AND PF

I_{in} (A)	V_{in} (V)	$THDC$	PF
44.16	220	1.68	0.35

From Fig. 4, Fig. 5 and Table II can be concluded that the input current in the full-bridge AC/DC converter has greater total harmonic distortion and this converter operates with small power factor.

In Table III are given values for the input power P_{in} , output power P_{out} , output current I_o , output voltage V_o and converter efficiency η for different width of pulse of gate in IGBT transistors.

In the Fig. 6 is shown diagram for converter efficiency obtained from values given in Table III. From Table III and Fig. 6 can be concluded that maximum converter output power is 3.091 kW and maximum converter efficiency is 0.94 when the output power of the converter is maximum.

TABLE III: VALUES FOR P_{IN} , P_{OUT} , I_o , V_o AND η

pulse gate width	P_{in} (kW)	P_{out} (kW)	I_o (A)	V_o (V)	η
0-180°					
180°-360	3.29	3.09	124.40	25.00	0.94
0-150					
180-330	2.81	2.64	115.00	23.00	0.94
0-120					
180-300	1.79	1.67	91.20	18.24	0.93
0-100					
180-280	1.24	1.14	75.37	15.08	0.92
0-80					
180-260	0.78	0.71	59.43	11.88	0.91
0-60					
180-240	0.42	0.38	43.43	8.68	0.90
0-40					
180-220	0.18	0.16	28.55	5.71	0.90
0-20					
180-200	0.05	0.04	14.26	2.85	0.84
0-10					
180-190	0.01	0.01	7.11	1.42	0.71
0-10	0.00	0.00	0.00	0.00	0.00

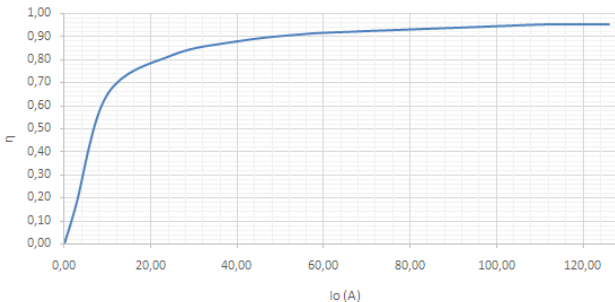


Fig. 6. Converter efficiency at the full-bridge AC/DC/DC power converter obtained by simulations.

4. Experimental Results

Based on the results obtained above practical prototype of the full-bridge AC/DC/DC power converter for arc welding is realized. The operation of the prototype is experimental tested and results are given here. The experiments are made for input mains voltage $V_{in} = 220$ V. The output no-load voltage is about 60 V, which is enough for arc burning at normal operating conditions. The maximum output power of the converter is 3.09 kW at switching frequency of 64 kHz. The prototype of practically realized convertor is shown on Fig. 7. The values of the converter elements are same as those used in the simulation phase. The properties of the converter were verified in arc welding application for full range of load current from no-load to short circuit.

Control circuit is realize by 8-bit microcontroller 16F877 Pic [13] with embedded microcontroller CCP (Capture /Compare / PWM) modules. Controller outputs generate pulse-width signals.



Fig. 7. Prototype of converter.

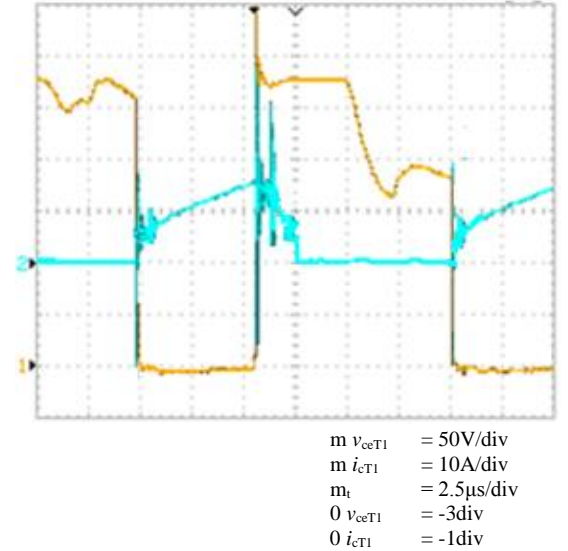


Fig. 7. v_{ceT1} and i_{cT1} of transistor T_1 .

The switch voltage v_{ceT1} (channel 1) and switch current i_{cT1} (channel2) of the transistor T_1 in the converter are shown in Fig. 8. The transistor is turned-on under zero-voltage switching. Because of symmetry of the leg the transistor T_4 works under the same operating conditions.

From Fig. 8 can be seen that the turn-on and turn-off losses are considerably reduced. Only the tail current of the transistor causes some turn-off losses. The detail of the turn-off transition is shown in Fig. 9.

Fig. 10 shows the dynamic properties of transition from short circuit to no- load of the converter.

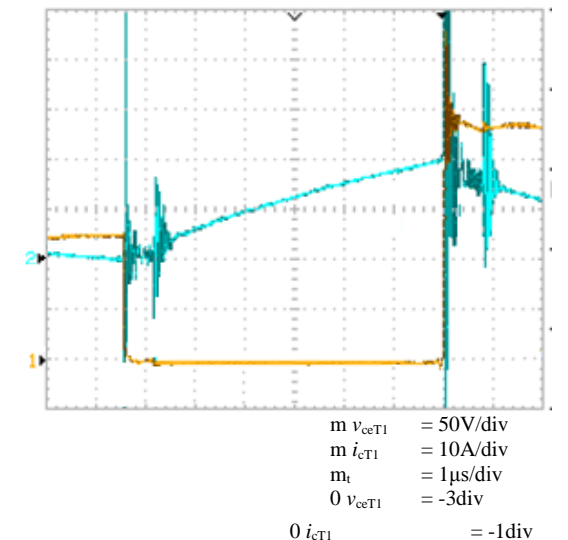
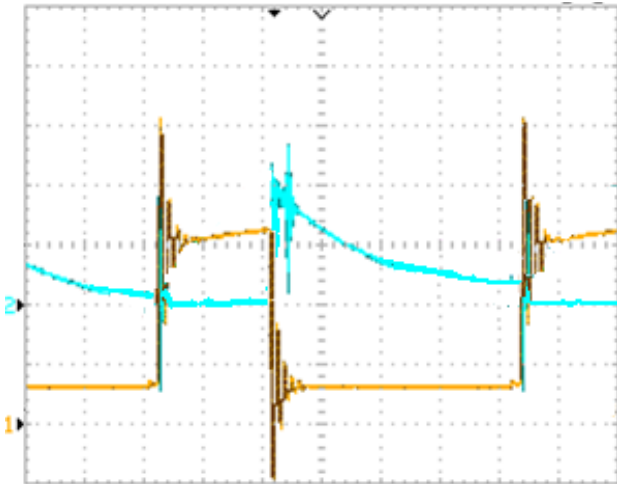


Fig. 8. v_{ceT1} and i_{cT1} of transistor T_1 -detail.

The measurement of the input variables of the converter is made with power analyzer CIRCUTOR CVM-NRG96NZ. In Table IV are given measured values on the effective input current I_{in} , input power P_{in} , total harmonic distortion of the input voltage $THDV$, total harmonic distortion of the input current $THDC$ and power factor P_{in} . This measurements are made for six set points.

TABLE IV: MEASURED VALUES FOR I_{in} , P_{in} , $THDV$, $THDC$ AND PF

No.	I_{in} (A)	P_{in} (kW)	$THDU$	$THDC$	PF
1	4.32	0.59	0.03	0.72	0.62
2	13.24	1.98	0.05	0.66	0.68
3	15.58	2.40	0.06	0.62	0.70
4	17,60	2.50	0.05	0.64	0.70
5	19,00	3.17	0.06	0.58	0.73
6	20,31	3.40	0.04	0.58	0.72



$m v_o = 20V/div$
 $m i_o = 50A/div$
 $m_t = 1\mu s/div$
 $0 v_o = -3div$
 $0 i_o = -1div$

Fig.9. v_o and i_o of the converter at short circuit, arc welding and no-load conditions.

From Table IV can be concluded that the total harmonic distortion of the input voltage $THDV$ is small and total harmonic distortion of the input current $THDC$ is high. Input power factor is in range from 0.62 to 0.73.

In Table V are given the measured values of the output current I_o , output voltage V_o and calculated values of the output power P_o , obtained together with measurements in Table IV. In Table V also are given data for converter efficiency $\eta = P_{out}/P_{in}$, calculated from values of the output and input power.

TABLE V: VALUES OF I_o , V_o , P_o AND η

No.	I_o (A)	U_o (V)	P_o (kW)	η
1	47.00	9.00	0.42	0.72
2	80.00	18.00	1.44	0.73
3	100.00	20.10	2.01	0.84
4	10,00	21.10	2.15	0.86
5	116.00	23.90	2.77	0.87
6	123.00	26.00	3.20	0.94

In Fig. 10 is shown diagram for converter efficiency obtained from values given in Table V.

From Fig. 10 can be seen that at nominal output power the efficiency of the converter is over 90 %. If the output power of the convertor is one half of the maximum output power than the efficiency convertor is greater than 75 %. Also, at minimal output power (0.42 kW) the efficiency of the convertor is greater than 70 %.

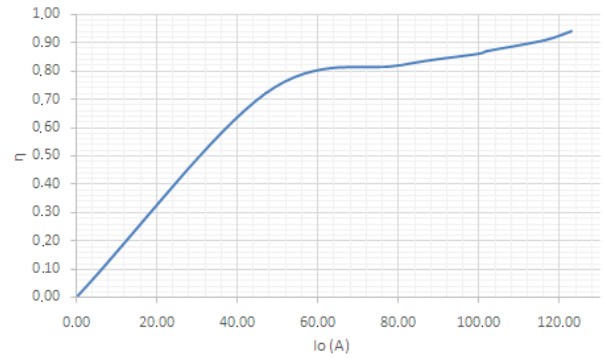


Fig. 10. Experimental obtained efficiency of the prototype of full-bridge DC/DC power converter at arc welding.

4. Conclusion

AC/DC/DC converters by Phase-Shifted PWM control is design and practical realize. Effect the tail current problem at turn-off the IGBT and their impact on the power losses is estimated with computer simulations.

The turn-off loss is reduced by capacitors, acting as the non-dissipative snubbers. Reduction of turn-on losses is achieved by using the leakage inductance of transformer.

The realized prototype is tested and obtained its input/output characteristics. The harmonics in input current and power factor, as and efficiency of the converter are determined.

Operation on high frequency allows reduction of the volume and weight of the converter.

5. References

- [1] W. B. Williams, Principles and Elements of Power Electronics, University of Strathclyde, Glasgow, 2006.
- [2] W. Shepherd, L. Zhang, *Power Converter Circuits*, Marcel Dekker, 2004, ch.15
- [3] D. Maksimovic, R. Zane, R. Erickson, "Impact of digital control in power electronics", In Proceedings of the IEEE 16th International Symposium on Power Semiconductor Devices and ICs. May: 13–22. 2004.
- [4] K. Harada, Analysis and Design of ZVS-PWM Half-Bridge Converter, IEEE PESC Record, 1995, pp. 280-285.
- [5] J. Shklovski, K. Janson, T. Sakkos, Natural Mode Constant Power Source for Manual Arc Welding, *Elektronika Ir Elektotekhnika*, Vol 18, No 9, 2012.
- [6] G. Hu, H. Lei, X. Ma, Constant Current Control of DC Electronic Load based on Boost Topology, *Elektronika Ir Elektotekhnika*, Vol.20 No.2, pp.36-39, 2014 [Online]. Available: <http://dx.doi.org/10.5755/j01.eee.20.2.6381>
- [7] J. Dudrik, Current Source for Arc Welding, *Elektro (journal)*, 1993, No.1, pp. 450-455 (in Slovak).
- [8] G. Stefanov, Lj. Karadzinov, B. Zlatanovska, Mathematical Calculation of H-Bridge IGBT Power Converter, *Comptes rendus de l'Academie bulgare des Sciences*, Volume 64, Issue No6, pp.897–904, 2011
- [9] PowerSim Software, <http://www.powersim.com/>
- [10] M. Horváth, J. Borka, Welding Technology and Up-to-date Energy Converters, EDPE 2005 Conference, Dubrovnik, Croatia, September 24–26, 2005. CD-Proc. E05-.
- [11] G D.C. Kim, H.J. Park, I.S. Hwang, M.J. Kang, Resistance spot welding of aluminum alloy sheet 5J32 using SCR type and inverter type power supplies, *International Scientific Journal*, Volume 38, Issue 1, Pages 55-60, July 2009.
- [12] H. Bissell, R. Boilard, "Selecting the Correct Size Inverter for DC Welding", *Welding Technology Corporation*.
- [13] PIC16F87X Data Sheet Microcontrollers, Microchip Technology Inc., USA, 2001.